The Effect of Abrasive Particles Movement on Deburring Effectiveness in REMF Process by using Explicit Dynamic Simulations

Jung-Hee Lee
Pukyong National University - Daeyeon Campus: Pukyong National University
Se-Yeong Lee
Pukyong National University - Daeyeon Campus: Pukyong National University
Jae-Seob Kwak (jskwak5@pknu.ac.kr)
Pukyong National University - Daeyeon Campus: Pukyong National University

Research Article

Keywords: Dynamic abrasive media behavior , Deburring effectiveness , Rotational electro-magnetic finishing , Explicit dynamic analysis , Response surface methodology

Posted Date: June 16th, 2021

DOI: https://doi.org/10.21203/rs.3.rs-585186/v1

The effect of abrasive particles movement on deburring effectiveness in REMF process by using explicit dynamic simulations

Jung-Hee Lee[1] · Se-Yeong Lee[1] · Jae-Seob Kwak[1]

Abstract

The main aim of this study was to suggest rotating electro-magnetic finishing(REMF) which had the capability to yield ultra-fine finished surface in micro-meter level with high productivity in a short time. The performance of the REMF process was primarily dependent upon magnetic and impact energy by the physical properties of a particle, particle velocity, and impact angle. Therefore, in this study, numerical simulations were conducted by explicit dynamic analysis to verify the effect of both single and multiple abrasive media impact characteristics on a deburring area of the machined surface. Based on the observed results and Pareto analysis, it was found that the overall weight of the particles was the most significantly affected for burr reduction, and deburring area was proportional to the increasing impact angle as well. In addition, to estimate the relationship between process factors and output variable and determine the optimum condition for burr reduction, a second-order polynomial model was developed by adopting a response surface methodology. As a result, the predictive model agreed with numerical analyzed results with 84.4% of the accuracy rate. The optimized deburring area was 2.27mm^2 at 1,800rpm of rotational velocity, 0.7mm of particle diameter, and 2.0kg of total particle weight. It was founded to be similar to the maximum deburring area, about 2.37mm^2, obtained from the simulations at the same condition.

Keywords Dynamic abrasive media behavior · Deburring effectiveness · Rotational electro-magnetic finishing · Explicit dynamic analysis · Response surface methodology

1 Introduction

With increasing miniaturized components in ultra-precision engineering fields such as optics, automobile, aerospace, electronics, and medicine, micro-machining processes that could rapidly manufacture high integrity parts have attracted attention for researchers in the past decades. Compared to diverse micro-machining methods, micro-milling is well established to simply create complex elements in small feature sizes with precision and accuracy[1]. Although this mechanical operation offers a lot of advantages it still has challenging tasks in terms of burr formation and surface defects due to direct contact between the cutting tool and workpiece. These unexpected parts on the machined surface adversely affect desired functionality, performance, and dimensional accuracy of the finished products[2, 3].

To cope with challenges encounter in typical micro -milling operation and achieve the fine surface with high quality, efforts to minimize burrs are necessary. Majority of researchers in both industries and academia have attempted to introduce effective post-processing strategies which are categorized into two main parts: traditional and advanced deburring processes. The former technologies, such as honing, lapping, and grinding, restrict access to the micro-structures and remove uneven materials due to the stiff movement of tools. As a result, these are now being replaced by the latter finishing processes as alternatives to overcome inherent limitations of conventional methods and achieve ultra-precision surface finish on the complex shape geometries[4, 5].

In particular, abrasive flow machining(AFM) and magnetic field assisted finishing methods, for instance, magneto-rheological abrasive flow finishing(MRAFF) and magnetic abrasive finishing(MAF) are considered to be promising precision finishing methods among the advanced techniques. Petare and Jain conducted experimental research on improvement in micrometric surface finish, dimensional accuracy, and wear characteristics of the straight bevel gear by applying AFM to ensure that AFM was the efficient and economical way to achieve the fine surface of internal morphology. As a result, reduction in surface roughness and micro-geometries with tight tolerance were proportional to finishing cycle time and media viscosity. Besides, it was found that low frictional heat caused by lower wear characteristics improved reliability, durability, and strength of the gears[6]. Baraiya et al. derived a novel fixture which allowed abrasive media to flow around both external and internal surfaces of ring-shaped Al6061 workpiece simultaneously and evaluated the influences of input variables on surface roughness. The results showed that the key feature of fine surface was the number of cycles, followed by abrasive concentration and abrasive mesh size[7]. Sankar et al. developed the improved viscoelastic abrasive-laden media to enhance the ability to fully remove surface peaks in the micrometric range. It was reported that blended

✉ Jae-Seob Kwak
Jskwak5@pknu.ac.kr

1 Department of Mechanical Engineering, Pukyong National University, Busan, 48547, Korea

styrene polymer which has elastic properties helped to increase radial force acting on abrasives so that it led to accelerating surface roughness reduction[8]. Kathiresan and Mohan studied MRAFF that combined both AFM and magneto-rheological finishing to perform high degree finishing with dimensional stability over the intricate SUS316L surface. This research not only set up predictive models of material removal rate(MRR) and surface roughness but also figured out optimal process parameters affecting desired values by the experimental approach and firefly algorithm. On the basis of a developed mathematical model, there was a good agreement between observed and predicted results[9, 10]. Jayant and Jain attempted to perform numerical analysis of magnetic flux density, flow characteristics, and MRR which affected the ultra-fine finished surface of an asymmetric medical implant in the MRAFF process for predicting the final surface state accurately. The developed model, taking into account the number of abrasives and their distribution, was close to the experimental results with the acceptable accuracy[11]. Li et al. applied viscoelastic abrasive media instead of powder mixture commonly used in the MAF process and optimized polarity arrangement by applying finite element analysis(FEA) to improve finishing efficiency and surface integrity. Based on the determined array, the experiments were conducted to validate theoretical models for change in surface roughness and MRR. Consequently, it showed that both responses had a strong relationship with experimental results within 5% of the error rate [12]. During the MAF process, surface topography was negatively affected by excessive temperature due to relative motion between the finishing zone and active abrasive media. Singh et al. formulated the predictive temperature model that considered critical process parameters and thermo-physical properties of workpieces. In comparison with experimentation, the temperature model was validated and it was revealed that important parameters for the surface finish were voltage and the weight ratio of abrasive particles[13]. Even though these developed technologies were preferable to traditional ones in terms of irregular surface morphology and inaccessible areas, it was still limited in mass production due to low productivity, high finishing cost, and non-uniform abrasive force.

Therefore, this study presents rotational electromagnetic finishing(REMF) as one of the advanced abrasive finishing processes which utilizes magnetic and kinetic energy exerted by massive abrasives for efficient deburring. Yoshioka et al. recorded motion of abrasive particles by using a high-speed camera. The behavior of abrasive particles was subject to revolution and rotation in the presence of the rotating magnetic field. From the analysis of active abrasives, kinetic energy for excellent surface integrity was mainly affected by particle shape and size as well as rotational speed of magnets[14]. Zhang et al. proposed alternating magnet arrangement in both the plane and vertical axis to achieve superior surface performance[15]. Safavi et al. investigated the effects of machining parameters in the REMF process on surface roughness and found the optimum condition within the considered ranges[16]. Lee and Kwak performed experiments by the Taguchi orthogonal method to analyze the correlation between particles behavior and non-ferrous surface improvement as well as between working time and surface state. As a result, it was found that surface roughness improved by 50% from the initial state at the optimal condition[17]. From the conducted literature reviews, there have been few studies regarding the REMF process so far and these focused intensively on the experimental approach, which aimed to enhance surfacee integrity on the complex geometry shapes.

Thus, this study analyzes the dynamic behavior of abrasives in the fluid region to investigate the effect of abrasive movement with its physical properties on burr reduction by adopting explicit dynamic simulations. Based on the simulated results, a mathematical model would be derived to predict the deburring area on the target surface, which determines the degree of micro-sized burr removal, by response surface methodology(RSM). Furthermore, optimal process parameters are defined to yield the best performance on surface topography.

2 Mechanism of REMF process and particles behavior

The basic operation of REMF depends on magnetic and kinetic energy acting on abrasive particles as multi-point cutting tools in the presence of the alternating magnetic field. Both combined elements directly influence particle movement quantitatively, and hence it results in collision between active particles and surface peaks on the workpiece. Based on the collision effect, REMF has the ability to remove debris particles and improve quality efficiently on the machined surface, especially in difficult-to-access areas.

Fig. 1 depicts a schematic design of the REMF process based on an actual apparatus. It is mainly

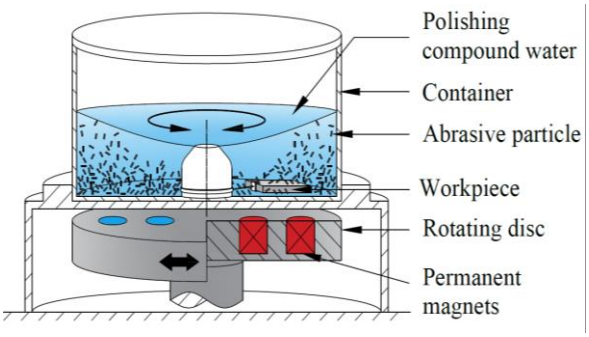

Fig. 1 Schematic diagram of the REMF process

composed of a fixed container, a rotating disc with permanent magnets, and a disc rotational velocity controller. The region of the fixed container in which deburring operation occurs contains workpiece, abrasive particles, and polishing compound diluted with water. Fig. 2 illustrates a principle mechanism of particle movement. The abrasive particles in the fluid flow are magnetized under the alternating magnetic field(H) induced by rotating permanent magnets so that it has different magnetic dipoles($+p$ or $-p$) at the end of each particle. Abrasive particles placed in the magnetic field are attracted toward magnetic lines of force due to magnetic force(F_p). This derived attractive force causes abrasive particles to turn in a circle during the process, as the magnetic field continuously changes along the direction of the rotating cylindrical disc. If the axis of abrasives are inclined at a certain angle(θ) to the magnetic field, the abrasive tool experiences a couple of force(F_m) at each pole. It leads to generating a couple of moment(T_p) on particles, and this phenomenon rotates magnetic abrasives along its own axis. Relevant equations of magnetic force and a couple of moment are explained as following Eq. (1) and Eq. (2).

$$F_p = \chi VH \cdot \Delta H \tag{1}$$

$$F_m = qH$$
$$T_p = F_m l \sin\theta = qlH \sin\theta \tag{2}$$

where χ and V are susceptibility and volume of the abrasive particle respectively. l represents length of abrasive particle.

Kinetic energy acting on dynamic abrasives, which have revolutionary and rotational movement experienced by magnetic force and torque, is given as Eq. (3). Thus, the motion of abrasive particles with kinetic and magnetic energy accelerates collision with the workpiece for the smooth surface.

$$E_k = E_{k,revolution} + E_{k,rotation} = \frac{1}{2}\left(Mv^2 + Iw^2\right) \tag{3}$$

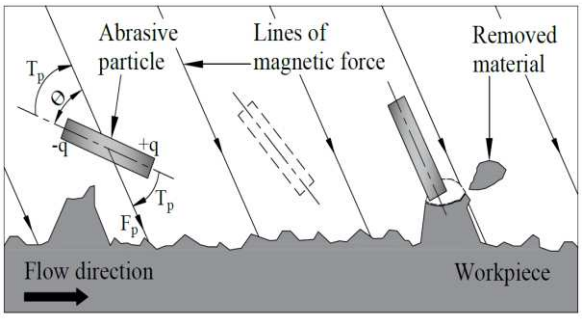

Fig. 2 Principle of particles movement

where M is particle mass, v is particle velocity, I is the moment of inertia, and w is angular velocity.

3 Simulation methodology and conditions

According to the equations in chapter 2, it can be inferred that the collision effect between magnetized abrasives and workpiece for accurate geometries of structures is tightly related to magnetic characteristics and abrasive particle properties. However, there are numerous process parameters affecting burr removal in this suggested finishing method, so it is impractical to perform experiments under all conditions. Thus, this study attempts to analyze the effect of violent motions of active abrasive particles in fluid flow on deburring performance by employing explicit dynamic simulations, In addition, the material removal areas of the targeted surface are predicted and optimized based on the simulated results. Since a number of particles contact with each other and workpiece simultaneously during the deburring task, it is difficult to specify the behavior of all the particles which includes positions, arrangements, tilted angle, and so force. Thus, this study evaluates the degree of stress distribution on the workpiece surface first, which indicates that a collision event resulted from single particle movement occurs to establish the reliable model for burr reduction in the suggested numerical strategy. Moreover, simulations of multi-particles movement are conducted based on the individual particle collision results to derive the deburring area over the yield stress of the workpiece. From the conducted results, the mathematical predictive model for fine finishing is developed by RSM.

To simplify the interactive mechanism between abrasive media and workpiece in this advanced finishing process, underlying assumptions are made as follows:

- All the abrasive particles are regarded as cylindrical in shape with the constant length of 3mm.
- Workpiece remains stationary where the magnitude of magnetic flux density reaches the maximum during the process, and it has identical yield strength everywhere.
- Distribution of magnetic flux density over the concerned surface area and abrasive media is uniform.
- There are no changes in the properties of the workpiece and abrasives during the finishing process.
- To avoid computational complexity, this study focuses on the effect of interaction between abrasives and workpiece surface, so collision between abrasive particles is negligible.
- Velocity of abrasive media is assumed to be the same as rotating speed of the cylindrical disc equipped with permanent magnets.

Materials of cylindrical shaped particles and workpiece are SUS304 and Al6061 respectively. In order to determine position of workpiece and abrasives' behavior, fundamental simulations are carried out by employing ANSYS workbench based on the actual apparatus(EMD-850L, Amech). The container as the finishing area has ϕ730mm of diameter and 300mm of height. In addition, four pieces of square-shaped Nd-Fe-B permanent magnets embedded into the rotating disc are alternatively arranged as NSNS. Fig. 3 shows the distribution of magnetic flux density in the conducted finishing area. To obtain a high quality of the surface, the workpiece is laid on the bottom of the container at 180mm of radial distance from the center of the equipment, which records maximum magnetic flux density of approximately 70.8mT. Considering length and diameter of magnetized abrasives, interested volume of the workpiece in this analysis model is designated as $5 \times 5 \times 2\text{mm}^3$. Since radial distance is quite longer than the width of the interested area, abrasive media are subject to linear transportation against the 2D plane of the workpiece shown in Fig. 4.

3.1 Single particle collision analysis

In the REMF process, burr reduction with high quality of surface topography takes place by a magnitude of impact energy between abrasive particles and the workpiece surface in the form of magnetic field. Thus, it is important to clarify behavior characteristics of abrasive media which affect deburring performance. To completely understand quantitative correlation between finishing performance and abrasive particles movement exerted by magnetic and kinetic energy, two steps of numerical simulations with Steinberg-Guinan strength model are examined by the explicit dynamic method. In the first step, the effects of individual particle collision on stress distribution of the surface are investigated under varying process factors and levels.

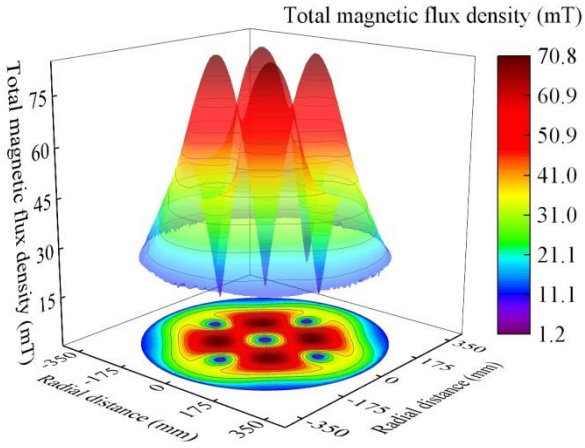

Fig. 3 Distribution of magnetic flux density in the finishing area

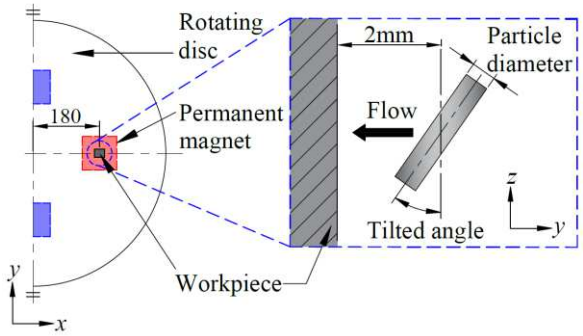

Fig. 4 Collision area between workpiece and particle

The modeling of workpiece and cylindrical shaped particle is created by UG NX11. Meshes of each modeling are generated with the help of ANSYS workbench as represented in Fig. 5. The mesh size of the collision area that directly influences the finishing performance is denser than other areas to obtain reliable results with minimum errors and to reduce the computational time. During the analysis, the abrasive particle as a rigid structure delivers kinetic energy to the surface without any deformation, while the workpiece is regarded as a deformable body.

As can be seen in Eq. (3), it is inferred that kinetic energy is tightly related to weight and velocity of particles, so independent input variables including rotational velocity, particle diameter, and impact angle with corresponding levels are determined as listed in Table 1. The range of rotational speed varies from 1,200rpm to 1,800rpm based on trial experiments and manufactured in-house apparatus setup in order to effectively perform material removal. The lower and upper limits of particle diameter are 0.3 mm and 0.7mm respectively. This is because that diameter exceeding 0.7mm causes surface defects

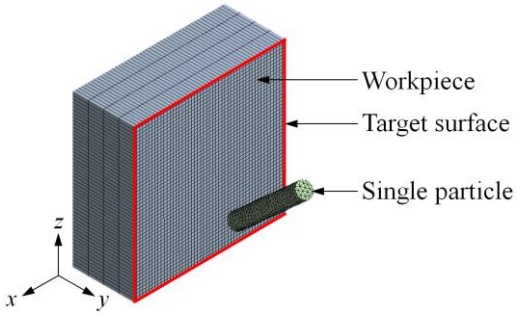

Fig. 5 Simulated model for single particle collision

Table 1 Process parameters for simulations

Process parameters	Levels		
	1	2	3
Rotational speed(rpm), A	1,200	1,500	1,800
Particle diameter(mm), B	0.3	0.5	0.7
Tilted angle(°), C		0 - 90	

due to excessive force. On the other hand, it shows few effects on surface finish less than 0.3mm. Tilted angle defines angle between the center of the workpiece surface and the middle point of particle along the axial direction. It ranges from 0° to 90° with 3°increments. For instance, 0° of incident angle represents that the abrasive particle is parallel to the surface, whereas it is perpendicular to the surface at 90° of angle. Moreover, standoff distance between both materials is constant, about 2mm. Based on the given conditions, stress distribution analysis is performed by full factorial design of experiments to investigate the effects of single object behavior on surface finish.

3.2 Multi-particles collision analysis

In practice, burrs generated on the machined surface are able to be reduced by the interaction mechanism between the workpiece surface and multiple abrasive particles. Therefore, in order to obtain realistic results from numerical analysis, it needs to clarify the burr removal mechanism in this complicated finishing phenomenon. In this stage, it is assumed that the existence of burrs on the machined ductile materials is successfully removed when von-Mises stress acting on the surface by multiple particles movement is over the yield stress. In this study, the yield stress of Al6061 is about 276MPa.

The process parameters and fixed conditions affecting particles behavior are identical to the former analysis shown in Table 1. Moreover, total particle weight as a process factor D is designed additionally in a range from 1.0kg to 2.0kg to determine the number of active particles participating in the collision event. The number of active particles contacted to the target surface is calculated by the proportional equation given in Eq. (4). The distribution of all the media in the interested area regards to be uniform, and multiple particles reach the surface simultaneously in a short time, about 1×10^{-4}s.

$$N_i = \frac{W_t B_a h_a}{V \rho B_t H_t} \tag{4}$$

where N_i is the number of particles, W_t is total weight of particles, V denotes particle volume calculated by given length and diameter, ρ is density of the abrasive particle. B_t and H_t represent total magnetic field and total compound liquid height in the cylindrical container which is a part of the equipment respectively. B_a and h_a are magnetic field and surface height in the interested finishing area respectively.

Fig. 6 shows a flow diagram of how 27th multi-particles simulations are performed. Once a number of particles are calculated based on Eq. (4), relative positions in the XZ plane and tilted angle for initial particle(N_1) are randomly generated, and initial values of (x_{N_1}, z_{N_1}) and a_{N_1} are saved. In the second step, a couple of vectors of the next individual are produced by the random number generator same as the first step, and then the distance of the two directional positions between new vectors(i) and previous ones($i-1$) is compared to determine whether their positions are overlapping each other or not. This is because that those particles have their own coordinates while the angle vector is repeatable within the range from 0° and 90° with 3° interval according to the underlying assumptions in Chapter 3. If the measurement value is between 0mm and particle diameter, the algorithm returns to the first to generate other vectors. Otherwise, the sets of P and A

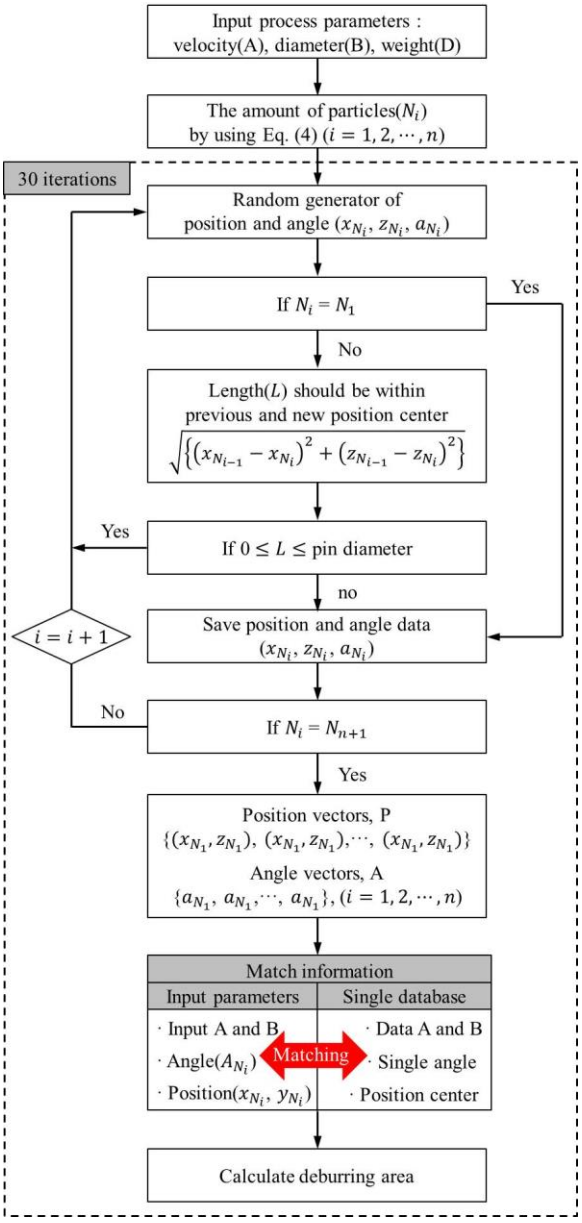

Fig. 6 Flowchart of multi-particle simulations

vectors which contain the n^{th} position and angle of the particle respectively are saved. After coordinates and incident angle of active particles are randomly designed, deburring areas are obtained by employing a data matching algorithm between single and multiple particles simulations to verify the effect of burr removal performance in the REMF process. First of all, stress distribution resulted from the individual particle analysis is loaded and compared to conditions of multi-particles simulations by means of one-to-one correspondence in terms of rotational speed and pin diameter as input process variables as well as tilted angle. Extracted von-Mises stress datasets of each individual are put into the center position of (x_{N_i}, z_{N_i}) in the target region, and then it adds up to calculate the deburring area where the sum of stress values is over 276MPa.

4. Simulation results and discussion

4.1 Single particle collision effect

In single particle behavior simulations, the distribution of equivalent von-Mises stress, which was a criterion of burr removal was examined in all 279^{th} possible scenarios by explicit dynamic FEA considering rotational speed, pin diameter, and incident angle to analyze the effect of the single magnetized particle impact characteristics on removing unexpected parts on the surface. Fig. 7 showed the number of elements where the stress values were over the yield stress of Al6061, about 276MP, without surface fracture. As can be seen, the main findings in this numerical analysis were that the effective collision areas were exhibited at larger particle diameter and higher particle velocity corresponding to 0.7mm and 1,800rpm, respectively. In contrast, relatively smaller diameter and lower speed had less chance to collide with the workpiece surface during the REMF process. This was because that kinetic energy acting on the particle, which was responsible for successful deburring, mainly depended upon the physical property related to the particle volume and rotational speed. Hence, the dynamic particle motion subject to higher kinetic energy was expected to result in material removal on the interested region.

From the Fig. 8(a), the minimum stress distribution was at 1,200rpm of rotational speed, 0.3mm of particle diameter, and 0° of impact angle. On the other hand, maximum value showed at 1,800rpm, 0.7mm, and 81° as represented in Fig. 8(b). It was observed that impact angle was also one of the dominant parameters for process efficiency, and impact energy acting on the target material tended to gradually increase with increasing tilted angle. This was because that magnetic torque applied on each particle was influenced by tilted angle between particle and magnetic field axis by Eq. (2). Thus, higher magnetic

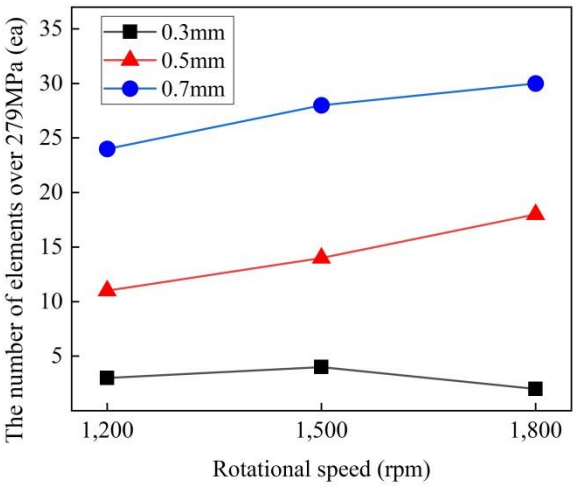

Fig. 7 The number of element over yield stress of 276MPa on the surface

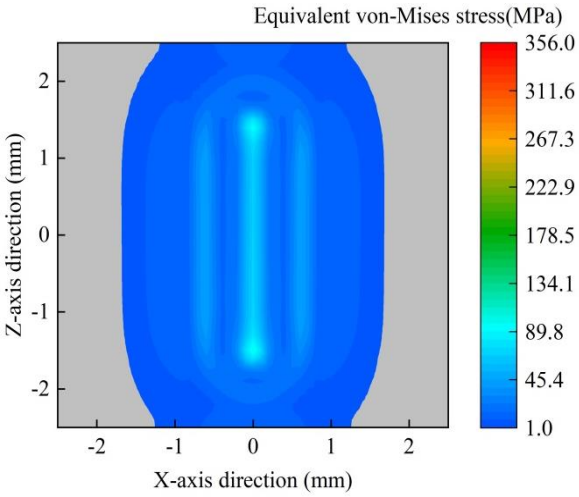

(**a**) Minimum stress distribution

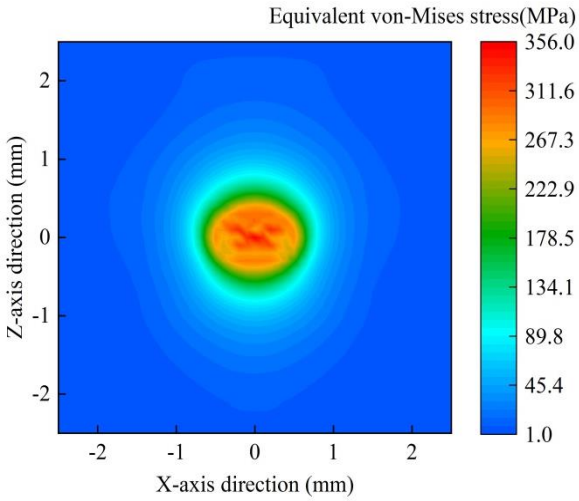

(**b**) Maximum stress distribution

Fig. 8 Computed equivalent von-Mises stress in single particle impact simulations

torque having a large amount of impact energy contributed to removing peaks of workpiece surface, while low magnetic energy was insufficient for effective deburring performance.

4.2 Multi-particles collision effect

In accordance with the simulation algorithm shown in Fig. 6, the 27th of multi-particles impact simulations were carried out by adopting explicit dynamic simulation taking into account rotational speed, particle diameter, particle weight, as well as varying impact angle. Each scenario was repeated 30 times to enhance the reliability of the suggested model with minimum errors. Fig. 9 showed the results in the relation of effective deburring area of the workpiece. In the former, the area beyond the yield stress was minimum as 0.21mm^2 at $A_1B_2D_1$ corresponding to 1,200rpm of rotational speed, 0.5mm of particle diameter, and 1.0kg of total particle weight, while maximum burr removal area was about 2.38mm^2 at $A_3B_3D_3$ which was 1,800rpm, 0.7mm, and 2.0kg in the latter. The results indicated that the effect of multiple particles movement on micro-sized materials removal was proportional to increase in particle velocity, diameter, and weight. In other words, process efficiency was influenced not only by kinetic energy generated by velocity and diameter of the particles, but also by total particle weight. It meant that increasing the number of particles involved in collision with the specific area of the workpiece achieved high quality of surface topography.

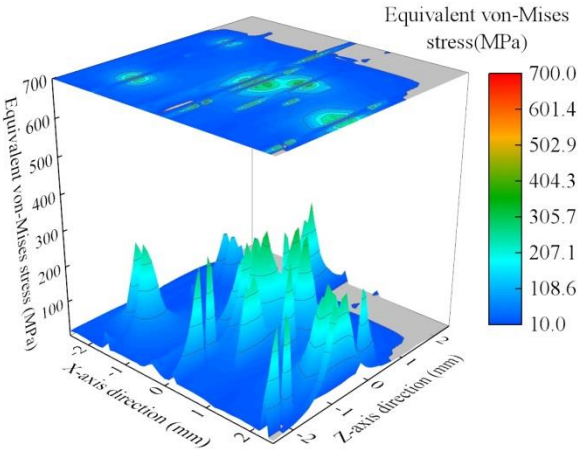

(**a**) Minimum deburring area

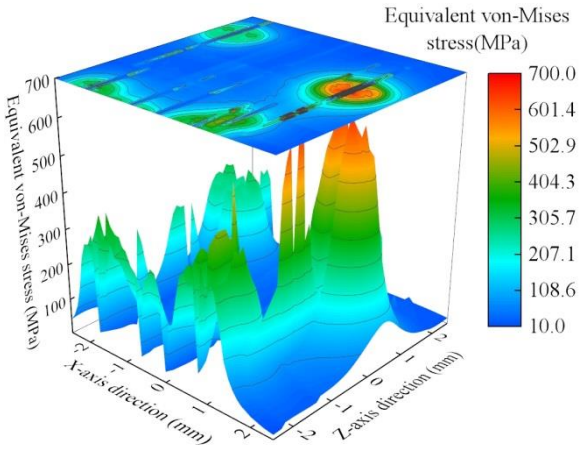

(**b**) Maximum deburring area

Fig. 9 Deburring area on the target surface resulted from multi-particles

In order to clarify significant parameters that influenced deburring efficiency in the REMF process, Pareto analysis was adopted at 95% of confidence interval as represented in Fig. 10. As can be seen, independent variables, interaction term between total particle weight and rotational speed, as well as quadratic particle diameter were statistically significant where the bars exceeded 2.08 of t-value corresponding to 95% of confidence level. Other interactions and square terms had proven inefficient. Among the significant factors, the number of active particles was the great effect on burr removal in micrometric surface finish followed by rotational speed, interaction between particle weight and rotational speed, quadratic diameter, and particle diameter.

Based on the Pareto analysis, a second-order polynomial regression model was developed by adopting RSM to predict the relationship between input variables and response as well as to optimize the output variable. The generalized quadratic equation was defined as follows.

$$\hat{y} = \beta_0 + \sum_{i=1}^{n} \beta_i x_i + \sum_{i=1}^{n} \beta_{ii} x_i^2 + \sum_{1 \le i < j}^{n} \beta_{ij} x_i x_j + e_{ij} \quad (5)$$

where $\hat{y}$ is dependent variable, β_0 represents the intercept constant, β_i denotes liner regression coefficients, β_{ii}, and β_{ij} are square and interaction of

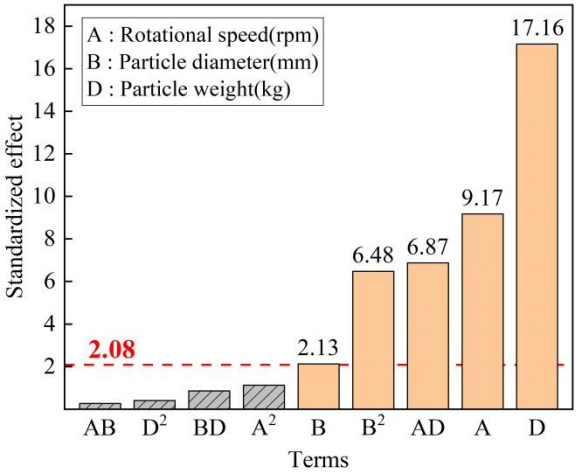

Fig. 10 Pareto chart for deburring effect

regression coefficients terms respectively. x_i and x_j are independent variables, i is the number of independent variables($n=3$, in this study). e_{ij} is the random error.

Eq. (6) was developed as the quadratic polynomial model in this study, considering significant input factors to reduce computationally time-consuming.

$$Area_{deburring} = 1.40 - 0.25A - 1.41B + 0.01D + 0.37B^2 + 0.28AD \quad (6)$$

In the derived model for deburring area, coefficient of determination(R^2) was 0.957 and adjusted R^2 was 0.947. Both values were close to 1 so that the predicted values were validated in good-agreement with simulated data. Thus, the accuracy rate between simulated and predictive results was about 83.3% as plotted in Fig. 11.

ANOVA analysis for the fitted model was listed in Table 2, and the trend was equal to the analyzed results from the Pareto chart. It was noticeable that probability value for all the selected factors was less than 0.05, which implied that considered parameters had the significant effect on deburring. Besides, the number of particles contributed to the largest influence had the significant effect on deburring. Besides, the number of particles contributed to the largest influence on the response with 59.7%.

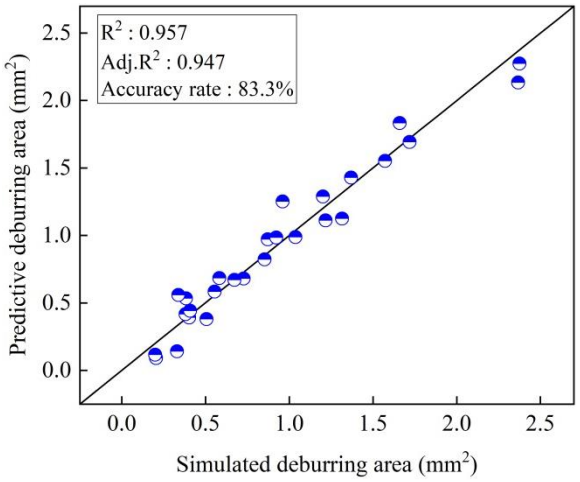

Fig. 11 Correlation between simulated and predicted deburring area

Table 2 ANOVA and statistical parameters of predictive regression model

Terms	DF	SS	MS	F-value	P-value
A	1	1.66	1.66	84.14	0.000
B	1	5.79	5.79	294.46	0.045
D	1	0.09	0.09	4.54	0.000
B^2	1	0.83	0.83	41.93	0.000
AD	1	0.93	0.93	47.17	0.000
Error	21	0.41	0.02		
Total	26	9.71			

Fig. 12 showed 3D surface plots for the deburring

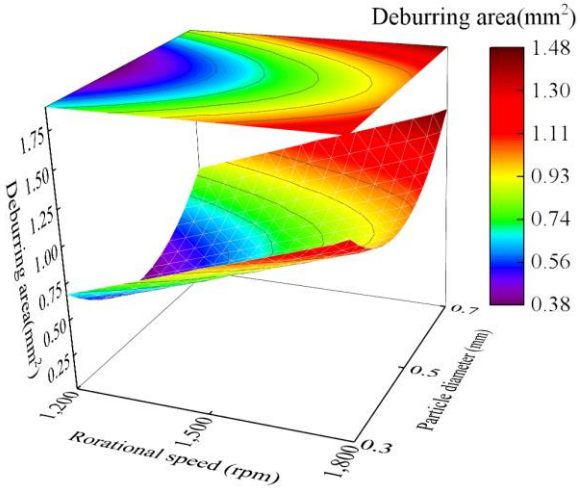

(**a**) Effect of rotational speed and particle diameter

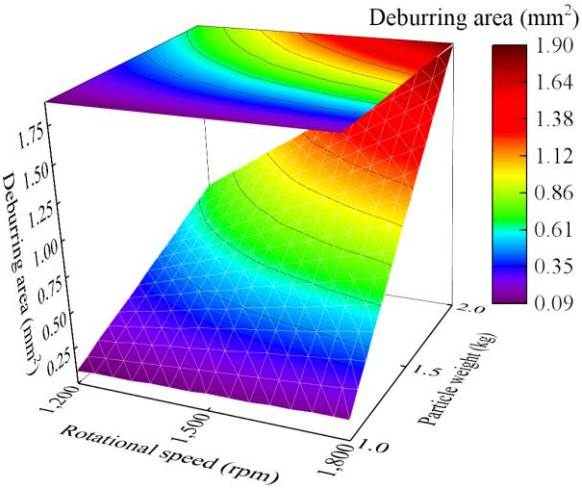

(**b**) Effect of rotational speed and particle weight

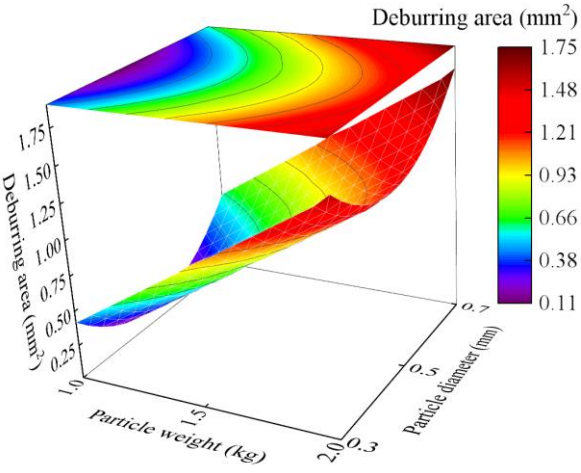

(**c**) Effect of particle diameter and particle weight

Fig. 12 Response surface plots for deburring area

area as a function of rotational speed, particle diameter, and particle weight. From Fig. 12(a), response linearly increased with increasing speed related to particle rotation, while particle diameter had the square effect on the deburring area. In addition, the slop of the amount of particles was quite steep compared to other parameters as shown in Fig. 12(b) and Fig. 12(c). This analysis agreed with the Pareto chart and ANOVA results as well. According to the results, optimized process factors where response yielded the highest material removal were set up at 1,800rpm, 0.7mm, and 2.0kg. At the determined condition, the optimum value was about 2.27mm^2. It was noted that the error rate was 4.6% compared to predictive results about 2.38mm^2.

5 Conclusions

In this study, the REMF process as the effective surface finishing method was proposed. To validate the effectiveness of this novel process for burr removal, the effect of abrasive particles movement on deburring performance was analyzed by using the numerical approach. Furthermore, RSM was adopted to develop the mathematical model for predicting the deburring area and derive the optimal condition for maximum burr reduction on the target surface. The main observations of this study were summarized as follows.

- In the REMF process, undesired materials on the machined surface were removed by collision between abrasive particles and the workpiece surface. Therefore, the dynamic abrasive particles motion exerted by magnetic and kinetic energy was the most important for process efficiency.
- In single particle impact simulations, the minimum stress distribution was at 1,200rpm, 0.3mm, and 0°, while the maximum value was observed at 1,800rpm, 0.7mm, and 81°. It was found that the deburring area, which was over 276MPa of Al6061 yield stress was proportional to increasing diameter and rotational speed of particles as well as impact angle.
- In multi-particle behavior simulations, maximum deburring area was 2.38mm^2 at 1,800rpm, 0.7mm, and 2.0kg. It was 10 times higher than minimum value of about 0.21mm^2 at 1,200rpm, 0.5mm, and 1.0kg. As can be seen, there was similar trend to the analyzed results from the single particle impact simulations.
- Based on the Pareto analysis, the significant input variable was total weight of particles, particle velocity, interaction term between total weight and particle velocity, squared particle diameter, and individual particle diameter, whereas other interaction and square terms were insignificant.
- The second-order polynomial model was developed by RSM not only to predict deburring area within considered factors and levels but also to figure out the relationship between response and process parameters. According to the results, derived model was fitted to simulated results with the higher R^2 and adjusted R^2 values corresponding to 0.957 and 0.947 respectively.
- The optimum condition for successful burr removal was 1,800rpm, 0.7mm, and 2.0kg. It was equal to the maximum deburring area condition resulted from multiple particles impact analysis. Compared to the deburring area between both results, the accuracy rate was 95.4%.

Declarations

Funding No funding was received for conducting this study.

Conflict of interest All authors had no conflicts of interest to declare that were relevant to the content of this article.

Data availability All the data supporting the results of this study were available within the article.

Code availability The modeling and simulations were conducted by UG NX11 and Ansys workbench.

Author's contributions Lee JH and Lee SY performed simulations and data analysis. In addition, they contributed to writing the paper. Kwak JS supervised the project and reviewed the paper.

Ethics approval Not applicable.

Consent to participate Not applicable.

Consent for publication All authors gave consent for publication.

References

1. Balázs BZ, Geier N, Takác M, Davim JP(2021) A review on micro-milling: recent advances and future trends. The Int J of Adv Manuf Technol 112:655-684. https://doi.org/10.1007/s00170-020-06445-w
2. Chen L, Deng D. Pi G, Huang X, Zhou W, (2020) Burr formation and surface roughness characteristics in micro-milling of microchannels. The Int J of Adv Manuf Technol 111:1277-1290. https:doi.org/10.1007/s00170-020-06170-4
3. Medossi F, Sorgato M, Bruschi S, Savio E (2018) Novel method for burrs quantitative evaluation in micro-milling. Precision Engineering 54:379-387. https:doi.org/10.1016/j.precsioneng.2018.07.007
4. Zou Y, Xie H, Dong C, Wu J (2018) Study on complex micro surface finishing of alumina ce-

ramic by the magnetic abrasive finishing process using alternating magnetic field, The Int J of Adv Manuf Technol 97(5):2193-2202. https://doi.org/10.1007/s00170-018-2064-0
5. Wei H, Gao H, Wang X (2019) Development of novel guar gum hydrogel based media for abrasive flow machining: shear-thickening behavior and finishing performance. Int J of Mech Sci 157:758-772. https://doi.org/10.1016/j.ijmecsci.2019.05.022
6. Petare AC, Jain NK (2018) On simultaneous improvement of wear characteristics, surface finish and mirogeomety of straight bevel gears by abrasive flow finishing process. Wear 404: 38-49. https://doi.org/10.1016/j.wear.2018.03.002
7. Baraiya R, Babbar A, Jain V, Gupta D (2020) In-situ simultaneous surface finishing using abrasive flow machining via novel fixture. J of Manuf Processes 50:266-278. https://doi.org/10.1016/j.jmapro.2019.12.051
8. Sankar MR, Jain VK, Rajurkar KP (2018) Nano-finishing studies using elastically dominant polymers blend abrasive flow finishing medium. Precedia CIRP 68:529-534. https://doi.org/10.1016/j.procir.2017.12.108
9. Kathiresan S, Mohan B (2018) Experimental analysis of magneto rheological abrasive flow finishing process on AISI stainless steel 316L. Material and Manuf Processes 33(4):422-432. https://doi.org/10.1080/10426914.2017.1279317
10. Kathiresan S, Mohan B (2020) Multi-objective optimization of magneto rheological abrasive flow nano finishing process on AISI stainless steel 316L. J of Nano Research, 63:98-111. https://doi.org/10.4028/www.scientific.net/JNanoR.63.98
11. Jayant and Jain VK (2019) Analysis of finishing forces and surface finish during magnetorheological abrasive flow finishing of asymmetric workpieces. J of Micromanufacturing 2(2):133-151. https://doi.org/10.1177/2516598418818260
12. Li W, Li X, Yang S, Li W (2018) A newly developed media for magnetic abrasive finishing process: material removal behavior and finishing performance. J of Materials Processing Technol 260:20-29. http://doi.org/10.1016/j.jmatprotec.2018.05.007
13. Singh RK, Gangwar S, Singh DK (2019) Experimental investigation on temperature-affected magnetic abrasive finishing of aluminum 6060. Materials and Manuf Processes 34(11):1274-1285. http://doi.org/10.1080/10426914.2019.1628263
14. Yoshioka M, Hira S, Takeuchi H (1999) Motion of magnetic barrel media in rotary magnetic field. Abrasive Technology: Current Development and Applications I 469-474. http://doi.org/10.1142/9789812817822_0063
15. Zhang Y, Yoshioka M, Hira S, Wang Z (2008) Effect of magnetic strength of three-dimensionally arranged magnetic barrel machine on polishing characteristics. Int J of Precision Eng and Manuf 9(2):34-38.
16. Safavi SM, Hasnavand S, Nedoushan RJ (2019) Experimental investigation of magnetic abrasive polishing of paramagnetic workpieces, Scientia Iranica B 25(2):785-795. https://doi.org/10.24200/sci2018.20415
17. Lee JH, Kwak JS (2020) Behavior characteristics of abrasive for improving surface integrity in magnetic pin polishing. J of Mech Sci and Technol 34(10):4069-4075. https://doi.org/10.1007/s12206-020-2218-5